Lattice Models for Confined Polymers

Jűrgen F. Stilck*
Instituto de Física
Universidade Federal Fluminense
Av. Litorânea, s/n 24210-340 - Niterói - RJ, Brazil

Received 26 October, 1998

Self-avoiding chains on regular lattices are frequently used as models to study thermodynamic properties of linear polymers, particularly regarding critical phenomena which may occur in these systems. We review these models, concentrating on their properties under geometric constraints, when the walks are placed inside strips or pores. In these cases the models may be solved using a transfer matrix formalism for the generating functions. A short range interaction between the sites visited by the walks and the walls is included in the model and the distribution of the sites and the forces on the walls are studied as functions of the strength of this interaction.
PACS: 05.50.+q, 61.41.+e

I Introduction

Polymers have attracted much interest for many years, basically because of the huge number of technical applications for them, but also due to some quite fundamental and challenging problems in the study of statistical mechanical models formulated to address their thermodynamical properties. Some of these models have been proposed and studied quite a long time ago [1], but interest in them was renewed as it was found that the models for polymers may present phase transitions analogous to the ones found in magnetic (and other) systems. Some of the simplest models for linear polymers represent them as self- and mutually-avoiding chains (the constraint takes care of the excluded volume effect), sometimes placed on a regular lattice. It is of interest to consider also other topologies for the polymer network [2], but here we will consider only linear chains. The formal equivalence of these models to the $n \to 0$ limit of an n-component spin model [3, 4] sheds light on this analogy. It also associates a hamiltonian to the model, since originally the models for polymers are among those models which may be called "geometric", in a sense that a statistical weight is associated to each allowed configuration of the lattice, but no hamiltonian is explicitly used in this connection. It is worth remarking that for n below 1 the n-vector model, viewed as a magnetic model, exhibits some anomalies, such as negative susceptibilities, and that some time ago its correspondence with polymer models has even be called into question [5], but a careful study of the equation of state in the scaling limit confirms the mapping [6]. Other examples of geometric models are the dimers [7] and percolation [8]. It is remarkable that for those models a correspondence to a hamiltonian model was also found, at least in some particular cases [9, 10].

To study the properties of self-avoiding walks on lattices, one may consider the partition or generating function

$$Y(x) = \sum C_{N,M} x^N y^M \tag{1}$$

where $C_{N,M}$ is the number of configurations of the lattice with M chains visiting a total of N sites of the lattice (sites incorporated into a chain will be called monomers). Physical systems which might be described by a partition function such as 1 are polymers in good solvents, since in this case one may neglect effective attractive interactions between the monomers induced by a poor solvent, which tend to drive the polymers into collapsed configurations, and only the excluded volume

*E-mail: jstilck@if.uff.br. On a leave from Departamento de Física, Universidade Federal de Santa Catarina.

interaction needs to be taken into account. Since the number of chains and the number of monomers in the polymeric chain may fluctuate, the partition function corresponds to the grand-canonical ensemble. Such a model, as stated above, may be mapped onto a magnetic n-vector model in the limit $n \to 0$, the activity of a monomer x being equal to the interaction term of the magnetic hamiltonian, while the activity y which controls the number of chains is proportional to the magnetic field term [11]. As usual for magnetic systems, in the limit $y \to 0$ the model undergoes a second order phase transition at a critical activity x_c in two or more dimensions. Unlike to what happens in the Ising model, in one dimension the model exhibits a first order transition at $x_c = 1$ [12]. The critical properties of the model, such as the critical activity and exponents, have been extensively studied by many techniques. In two dimensions, very precise results are known through transfer matrix calculations [13] and principally series expansions [14]. Also, the exact values of some critical exponents are known exactly in this case [15]. In the dilute limit, when interchain contacts may be neglected, one may consider the case of a *single* chain ($m = 1$ in Eq. 1). The problem of calculating the partition function, even in this particular case and on a two-dimensional lattice, has not been solved so far and there are indications that, if a exact solution might be found, it will not belong to the class of $D-finite$ functions, which encompasses all exact solutions known so far for statistical mechanical models [16].

The self avoidance constraint is the origin of the difficulty of solving the counting problems for chains on a lattice. If this constraint is relaxed (this is frequently called the *ideal* chain approximation), most of the calculations may be done analytically, but they result in classical critical exponents [4]. It is possible to take the excluded volume interactions into account partially, such as counting only chains without immediate returns. These calculations, although leading to better numerical values for non-universal parameters such as critical activities, also result in classical exponents, as expected. These "beyond mean field" approximations turn out to be equivalent to exact solutions of the models on treelike lattices, such as the Bethe and Husimi lattices [17]. Another simplified version of the walk counting problem are the so called *directed* walks, where it is assumed that in one or more axes of the lattice only steps in the *positive* direction are allowed [18]. Many analytical calculations are possible in such models, but again the correct critical exponents are missed. In Fig. 1 examples of some of the walks described above are depicted.

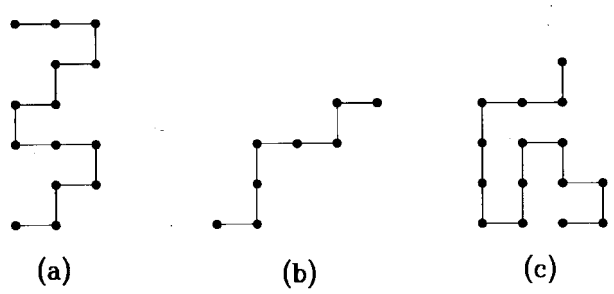

Figure 1. Examples of walks on the square lattice: (a) Partially directed walk, with positive steps only in the vertical direction; (b) Fully directed walk, with positive steps only in both directions; (c) Self-avoiding walk.

More recently, the behavior of polymers in the presence of a surface was studied [19], as was also done for other systems exhibiting critical phenomena [20]. An appropriate model for this problem consists in considering an additional Boltzmann factor $\omega = e^{-\beta\epsilon}$ for each monomer on the surface, so that $\epsilon < 0$ ($\omega > 1$) would correspond to an attracting surface. The partition function for this model is

$$Y(x,\omega) = \sum C_{N,N_w} x^N \omega^{N_w}, \qquad (2)$$

where the sum is over configurations of one chain with the initial monomer on the surface, N being the total number of monomers of this chain, N_w of them located on the surface. Actually, the behavior of polymers close to a surface has attracted the attention for quite a long time, and a thorough study for *ideal* chains [21] already showed that, if ω is above a critical value $\omega_0 > 1$, the surface polymerization transition will occur at a lower value of x than the one in the bulk. The phase diagram of this model is shown schematically in Fig. 2. It may be noted that for $\omega < \omega_0$ the polymerization transition occurs at the bulk critical value x_c and that this ordinary transition line O ends at the adsorption transition point A. This point is usually identified as a bicritical point [19], but it may have different characteristics for self-avoiding chains on a two-dimensional lattice limited by a line, since in this case we expect the surface transition S to be of first order, as happens for polymer models in one dimension with any finite width

[12, 22]. One possibility in this case would be that the adsorption transition corresponds to a tricritical point. This model and others related to it were much studied by several techniques such as scaling and Monte Carlo simulations [23], transfer matrix and finite size scaling methods [24] and series expansions [25].

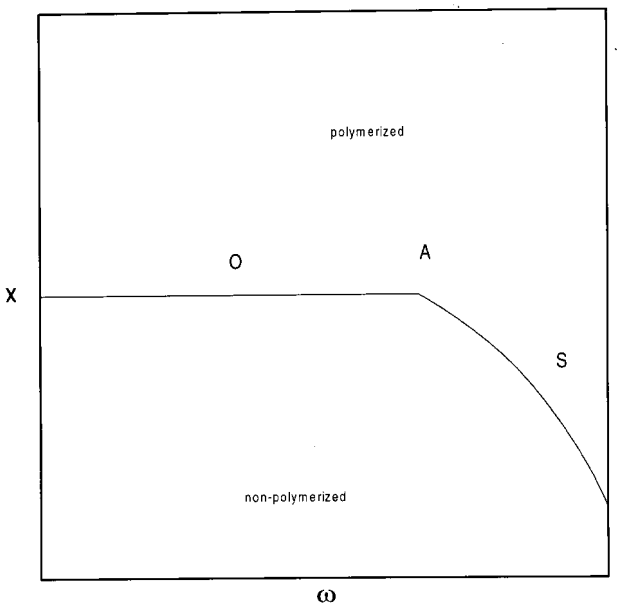

Figure 2. Phase diagram for a polymer in the presence of a surface. The activity of a monomer is denoted by x and a short range interaction energy ϵ for monomers located on the surface is included, so that $\omega = e^{-\beta\epsilon}$. O is the ordinary (bulk) polymerization transition, S is the surface polymerization transition and A is the adsorption multicritical point (also called special transition). A is located at $x = x_c$ (the bulk critical polymerization activity) and $\omega = \omega_0 > 1$.

The study of polymers in the presence of a surface leads naturally to the consideration of other geometric constraints, such as wedges and slabs [26]. In this paper we will review some recent work on the thermodynamic behavior of self-avoiding chain under a one dimensional constraint, such as a strip or a pore. In these cases the solution of the problem may be found through a recursive procedure for the generating functions of the model. In Section II we define the model and show the combination of transfer matrix and generating function formalisms which lead to its solution. The results for walks confined in strips are shown in Section III and some new results for walks in pores may be found in Section IV. Final comments and conclusions are in Section V. The spatial distribution of monomers and the tension on the walls for walks confined in a strip were already discussed before [27, 28].

II Definition of the model and its solution

We will consider self-avoiding chains which are confined in structures which are infinite in one direction (let us call it z) and finite in the direction(s) perpendicular to z. Two specific examples will be dealed with: a) A strip on the square lattice of finite width in one direction and infinite length, and b) A pore, with a finite crossection. Other geometries may also be considered, provided the number of lattice sites in the hyperplanes orthogonal to z is finite. If the sets of sites in each hyperplane are identical to each other, with respect to number and connectivity, as is the case in the examples above, the method of solution is simpler and we will consider this case from now on, assuming N_p sites in each of them. In general, we will allow the statistical weight of each monomer to be site-dependent, that is, its value will depend on the localization in the hyperplane of the site the monomer occupies. Thus there may be up to N_p different activities x_i, but in general we will be interested in more symmetric models and this number is reduced. The choice of different weights enables us to find the spacial distribution of monomers in the system and also to take into account interactions between the monomers and the walls, so that, for instance, a monomer which is located at the walls may have a different statistical weight than a monomer which is not. In order to take into account the excluded volume constraint, we follow the procedure proposed by Derrida [13] and specify, at each hyperplane, the connectivity properties of all bonds of the chain arriving from lower values of z. This may be done specifying the bond belonging to the segment of the chain which includes the initial monomer (placed at $z = 0$) and the pairs of bonds connected to each other by a segment whose monomers are all at lower values of z. In Fig. 3 these definitions are shown through examples. The configurations of the hyperplanes are represented by a set of integer numbers associated to each of the N_p sites. A site with no bond incident from below is associated to 0, the only site connected to the initial monomer corresponds to 1 and the pairs of sites connected to each other are designated by the same number larger than 1, different for each pair. The maximum number of possible configurations of a hyperplane is given by [29]

$$N_{c,max} = \sum_{i=0}^{\left[\frac{N_p+1}{2}\right]} J_i(N_p), \qquad (3)$$

where $J_i(N_p)$ is the number of configurations with i pairs, which is equal to

$$J_i(N_p) = \frac{N_p!}{i!(i+1)!(N_p-2i-1)!}. \qquad (4)$$

Actually some configurations do not occur due to boundary conditions and the self-avoidance constraint. For example, a configuration such as $(2,1,2)$ is forbidden for chains in a strip defined on the square lattice with a crossection of $N_p = 3$ sites and limited by walls impenetrable to the monomers. Also, the number of non-equivalent configurations is usually smaller due to the symmetry of the hyperplanes in each case. For example, for the strip with $N_p = 3$ the number of allowed configurations is $N_c = 5$ ($N_{c,max} = 6$ in this case), but due to the reflection symmetry this number will be reduced to $N_s = 3$, as is shown in Fig. 3. In any case, N_s increases very fast with N_p, and this sets a limit to the sizes of the crossections we are able to consider.

The partition function for confined self-avoiding chains may be calculated through a combination of the transfer matrix [13] and the generating function [18] formalisms. In order to obtain the partition function of an ensemble of confined self-avoiding chains, we first find the N_c allowed hyperplane configurations. Next, we define partial partition functions $g_z(k)$, which encompass the contributions of all monomers located below z and of chains which arrive at z in the k'th hyperplane configuration. Therefore

$$g_z(k) = \sum \prod_{i=1}^{N_a} [x_i^{N(i)}], \qquad (5)$$

where N_a is the number of different site dependent activities x_i and $N(i)$ is the number of monomers located below z of each walk considered in the sum. We thus have a set of N_c partition functions, and may consider the addition of an additional hyperplane to the walks included in $g_z(k)$. Since they all arrive at the hyperplane located at z in the k'th configuration, the partition functions g_{z+1} are related linearly to the g_z

$$g_{z+1}(i) = \sum_{j=1}^{N_c} A(i,j) g_z(j). \qquad (6)$$

The elements of the transfer matrix $A(i,j)$ are the contributions to the partition function of the monomers placed on the N_p sites located in the hyperplane at z. If configuration j may not be followed by configuration i, $A(i,j)$ is set equal to zero. In general, the elements of the transfer matrix are polynomials in the activities $x_i, i = 1, N_a$, one monomial for each possibility of having configurations i and j connected. We will choose the initial monomer of the walks to be placed at the hyperplane $z = 0$. If we now order the N_c hyperplane configurations in such a way that the first N_p correspond to having just one bond arriving at one site from below, such as the first three configurations in Fig. 3, we will have

$$g_0(k) = \begin{cases} 1, & \text{if } k \le N_p; \\ 0, & \text{otherwise.} \end{cases} \qquad (7)$$

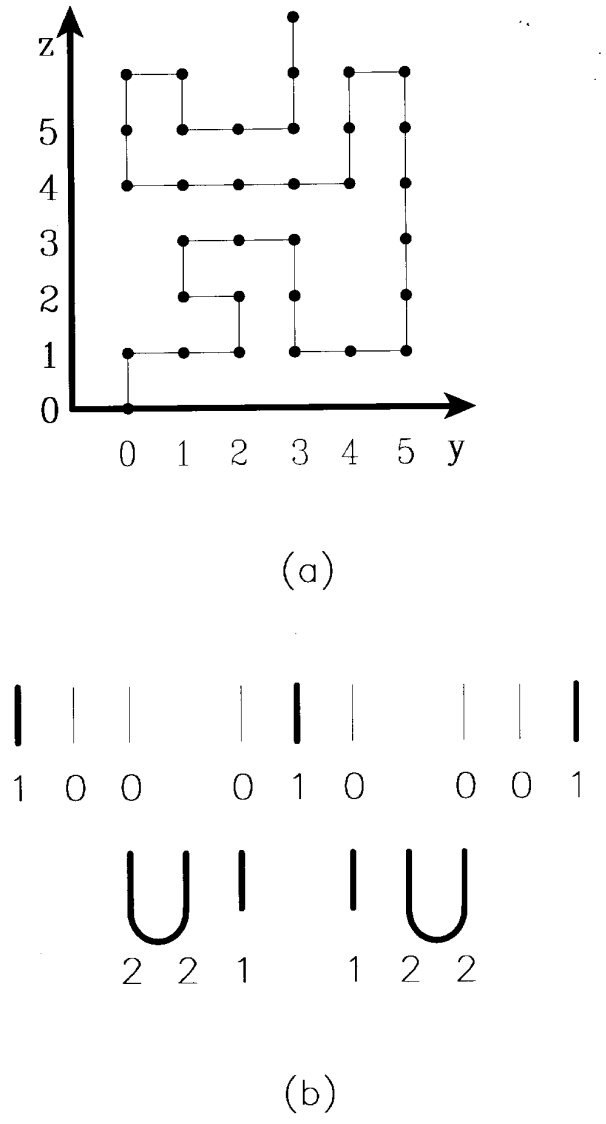

Figure 3. (a) - Self-avoiding walk confined in a strip with $N_p = 6$. The walk arrives at the line located at $z = 2$ in the configuration $(0,0,1,2,0,2)$ and at the line in $z = 6$ the configuration is labeled $(2,3,0,3,2,1)$. (b) - Allowed $N_c = 5$ line configurations for walks in a strip with $N_p = 3$ with the corresponding labeling indicated. Configurations $(1,0,0)$ and $(0,0,1)$ as well as $(2,2,1)$ and $(1,2,2)$ are related by reflection symmetry, and thus $N_s = 3$ in this case.

Considering now the ensemble of all the walks which end at *any* value of z in hyperplane configuration k, its partition function will be

$$G(k) = \sum_{z=1}^{\infty} g_z(k). \tag{8}$$

From the recursion relations for the partial partition functions, Equations 6, and the initial conditions on the walks which lead to Equations 7, we find that the partition functions $G(k)$ are the solutions of a set of N_c linear equations

$$\sum_{j=1}^{N_c} [A(i,j) - \delta_{i,j}] G(j) = -g_0(i), \tag{9}$$

where $\delta_{i,j}$ is the Kronecker delta. Calling B_i the matrices obtained if we replace the i'th column of the matrix $A \to A_I$ by the vector $-g_0$, the solution of these linear equations may be written as

$$G(i) = \frac{|B_i|}{|A - I|}, \tag{10}$$

where I is the identity matrix. Thus, the determination of the partition functions is reduced to the calculation of determinants. In general, due to the particular symmetry of the specific problem considered, the partition functions $G(i)$ will be equal for all hyperplane configurations related by symmetry. Thus, the actual size of the determinants we need to calculate in Equation 10 is reduced from N_c to N_s.

In general, we will be interested in a particular subset of the chains included in all the partition functions $G(i)$. For example, we might consider all chains which end at one of the first N_p hyperplane configurations. The appropriate partition function will be

$$G = \sum_{i=1}^{N_p} G(i). \tag{11}$$

The thermodynamic properties of the model may then be obtained from the partition function. For example, the mean number of the number of monomers with activity x_i in the chains will be

$$\langle N_i \rangle = \frac{x_i}{G} \frac{\partial G}{\partial x_i}, \tag{12}$$

and the mean number of monomers in the walk is

$$\langle N \rangle = \sum_{i=1}^{N_a} < N_i > . \tag{13}$$

Now expressions 10 and 11 for the partition function may be used and lead to

$$\langle N \rangle = \sum_{j=1}^{N_a} x_j \left(\frac{1}{\sum_{i=1}^{N_p} |B_i|} \frac{\partial \sum_{i=1}^{N_p} |B_i|}{\partial x_j} - \frac{1}{|A - I|} \frac{\partial |A - I|}{\partial x_j} \right). \tag{14}$$

At the polymerization transition the mean number of monomers diverges. In all particular cases we considered this divergence originates from the second term in Equation 14, so that $|A - I| \to 0$ is the critical condition. As expected, this condition is identical to the one obtained by considering a *single* chain using the usual transfer matrix formalism [13], which corresponds to having the largest eigenvalue of the transfer matrix A equal to 1. In our calculation, although an *ensemble* of chains is considered, the thermodynamic properties at the critical condition are dominated by the contributions of infinite chains at the polymerization transition. Another point to be stressed is that at the polymerization transition all thermodynamic properties are determined by the transfer matrix A, the contributions coming from the determinants $|B_i|$ vanish. This is physically very reasonable, since we would not expect that the initial and final conditions imposed on the walks, which are reflected in $|B_i|$, would have any influence on the transition. One quantity we consider is the fraction of monomers with a particular activity x_i, which is

$$\rho_i = \frac{\langle N_i \rangle}{\langle N \rangle}. \tag{15}$$

At the critical condition, this density is equal to

$$\rho_i = \frac{x_i \frac{\partial |A-I|}{\partial x_i}}{\sum_{j=1}^{N_a} x_j \frac{\partial |A-I|}{\partial x_j}}. \tag{16}$$

Finally, the tension or pressure applied by the chains on the walls which limit the strip or the pore may be calculated considering the change of the thermodynamic potential

$$\psi = -\frac{\ln(G)}{\beta} \tag{17}$$

as the walls are moved. This quantity diverges at the transition, so that the tension or pressure *per monomer* is the quantity to be looked at.

To do the calculations, we first generate all hyperplane configurations. Next, the transfer matrix is built, taking into account the symmetry of the model. These two first steps are done through computer programs with just logical and integer variables, the elements of the transfer matrix, which in general are polynomials in the activities, are calculated exactly. Finally, the transfer matrix is used as input for the numerical calculation of the thermodynamic properties of the model.

III Results for chains in strips

A particular realization of the calculations described above may be done for walks confined in strips defined on the square lattice. For a square lattice in the (y, z) plane, a strip with N_p sites in the crossection is defined by all lattice sites with $0 \leq y \leq N_p - 1$. This problem was already studied in detail for *ideal* chains [30], and it is interesting to find out what influence the self-avoidance constraint has on the results. A short range interaction between the monomers and the impenetrable walls located at $y = 0$ and $y = N_p - 1$ is included, so that a monomer located at the walls contributes with an additional Boltzmann factor $\omega = e^{-\beta\epsilon}$ to the partition function.

Due to the reflection symmetry of the model with respect to a line at $y = (N_p - 1)/2$, we start defining $[(N_p + 1)/2]$ activities, so that pairs of sites in the crossection which are equidistant of the center of the strip have the same activity. Without much computational effort, it was possible to study widths up to $N_p = 9$ ($N_c = 1353$ and $N_s = 681$ in this case). As an example, we give the transfer matrix for a strip with $N_p = 3$, with the crossection configurations ordered as in Fig. 3,

$$A = \begin{pmatrix} x_1 & x_1x_2 & x_1^2x_2 & 0 & x_1^2x_2 \\ x_1x_2 & x_2 & x_1x_2 & 0 & 0 \\ x_1^2x_2 & x_1x_2 & x_1 & x_1^2x_2 & 0 \\ x_1^2x_2 & 0 & 0 & x_1^2x_2 & 0 \\ 0 & 0 & x_1^2x_2 & 0 & x_1^2x_2 \end{pmatrix}, \tag{18}$$

where monomers in the center and on the walls have activities x_1 and x_2, respectively.

In this model, we studied the fraction ρ of monomers in each column y and the tension on the walls at the transition activity x_c for fixed values of ω. The critical activity is a decreasing function of ω for fixed width N_p. At low values of ω it decreases with N_p, whereas at higher ω an increase with N_p is obtained. The curves $x_c(\omega)$ cross the two-dimensional ($N_p \to \infty$) value for x_c roughly between 1.65 and 1.75. For ideal chains, the results are qualitatively similar, but all curves with $N_p \geq 2$ cross the two-dimensional critical activity value $x_c = 1/4$ at $\omega = 4/3$, which is the adsorption transition value for this case. For self-avoiding chains the adsorption transition is estimated to occur at $\omega_0 = 1.82 \pm 0.03$ [25], above the values in which $x_c(\omega, N_p)$ cross the two-dimensional critical activity. As N_p is increased, these crossing values increase also, approaching ω_0.

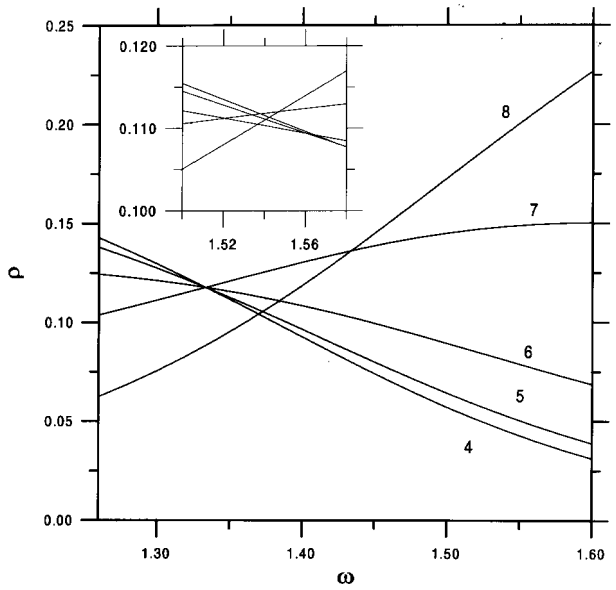

Figure 4. Fractions of monomers $\rho(y)$ located at column y for $N_p = 9$ as functions of ω. The main graph shows results for ideal chains and in the inset data for SAW's are shown. The curves are for y ranging from 4 to 8, as indicated.

The densities $\rho(y)$ show a concave profile for neutral walls $\omega = 1$, with a maximum density in the center of the strip. This is expected since the central region is favored entropically. As ω is increased, monomers on the walls decrease the energy of the system and thus the profile becomes convex. In Fig. 4 the densities are plotted as functions of ω for a strip with $N_p = 9$. Due to the reflection symmetry, $\rho(y) = \rho(N_p - 1 - y)$. For ideal chains, a flat profile in the internal columns

$(1 \leq y \leq 7)$is found when ω is equal to the adsorption value $\omega_0 = 4/3$, but the crossing pattern of the curves obtained for self-avoiding chains is more complex, as may be seen in the inset, and the profile in this case is convex at the estimated adsorption value for self-avoiding chains on the square lattice.

The force on the walls may be obtained through the procedure indicated above if we imagine the operation of increasing the spacing between the walls. If the lattice parameter is equal to a, we have

$$F = \frac{1}{a}\left(\frac{\partial \psi}{\partial y}\right) \tag{19}$$

where a attractive force is positive. As stated above, this force diverges at the polymerization transition, so that we consider an adimensional force per monomer, defined as $f = \frac{a\beta F}{\langle N \rangle}$, which may be calculated through

$$f = \frac{1}{x_c}\left(\frac{\partial x_c}{\partial N_p}\right)_{\omega} \tag{20}$$

Since we know the critical activities for integer values of the wall separation N_p only, we evaluate the derivative through a discrete approximation and thus

$$f(N_p + 1/2, \omega) = \frac{2[x_c(N_p+1,\omega) - x_c(N_p,\omega)]}{x_c(N_p+1,\omega) + x_c(N_p,\omega)}. \tag{21}$$

For ideal chains, the curves $f \times \omega$ may be seen in Fig. 5 for wall separation between 2.5 and 7.5. For $N_p \geq 2.5$ the force is repulsive for $\omega < \omega_0 = 4/3$ and attractive for ω above the adsorption value. For $N_p = 1.5$ the ω independent value $f = -2/5$ is found. Thus, for $\omega > 4/3$, a stable equilibrium point is found at low values of wall separation, an unstable equilibrium point being located at infinite separation. For ω below the adsorption value the force is always repulsive and the equilibrium point at infinite separation becomes stable. For self-avoiding chains, the situation changes qualitatively. The force vanishes at N_p dependent values of ω, all below the estimated adsorption value for this case, as may be seen in the inset of Fig. 5. This leads, for $\omega > 1.549375...$, besides the stable equilibrium point at low wall separation, to a new unstable equilibrium point at a finite value of N_p which grows as ω is increased. The equilibrium point at infinite separation is always stable. In Fig. 6 a curve $f \times N_p$ for self-avoiding chains is shown, illustrating the behavior described above. Thus, for self-avoiding chains, the rather unphysical behavior found for ideal chains, which show an attractive force between the walls for large distance above the adsorption transition, does not occur. More details about the behavior of chains in strips may be found in references [27] and [28].

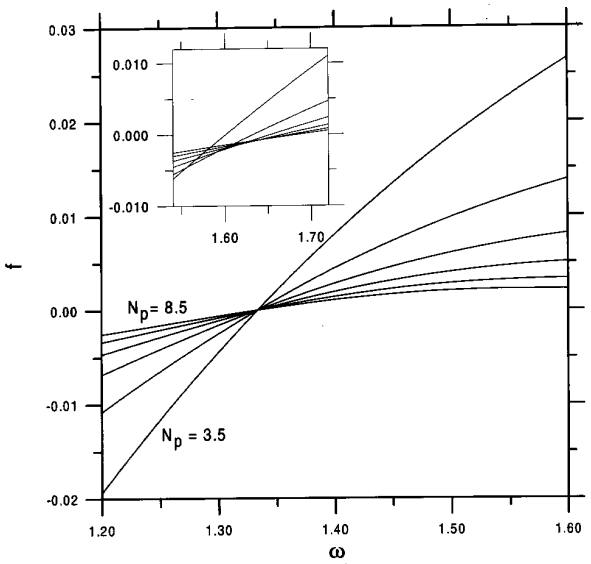

Figure 5. Force on the walls as functions of ω for ideal chains for values of N_p between 3.5 and 8.5. In the inset, results for self-avoiding chains and the same range for N_p close to $f = 0$ are displayed showing that, unlike to what happens for ideal chains, the force vanishes for different values of ω for each N_p.

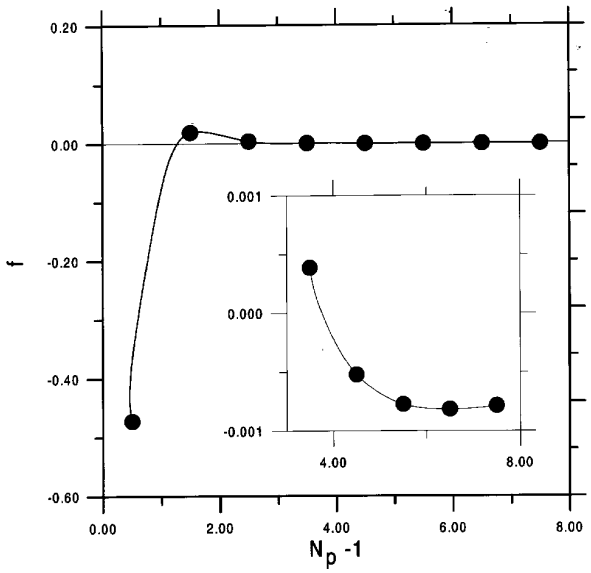

Figure 6. Force on the walls as functions of the wall separation $N_p - 1$ for self-avoiding chains and $\omega = 1.64$. The circles indicate the calculated values and the lines are just guides to the eye. In the inset, the region close to the unstable equilibrium point is enlarged.

IV Results for chains in pores

The generating function formalism using the transfer matrix can be used to study the properties of self-

avoiding chains in pores, with a finite crossection comprising N_p sites and infinite length in the z direction. Different crossections may be considered, such as squares and rectangles. To illustrate this, we will discuss here the problem of cylindrical pores, discretized so that the sites other than the central one are defined at r possible distances of the center and in m different directions, as may be seen in Fig. 7. In general, the number of sites in the crossection for a cylindrical pore defined as above will be $N_p = 1 + mr$. This is rather unphysical for large values of r, since we would expect N_p to grow with r^2. We number the sites sequentially in a way illustrated in Fig. 7. Due to the C_m symmetry of the problem, we define $r+1$ activities x_i, $i = 0, 1, \ldots, r$, for a monomer placed at distance i from the center. The force on the walls applied at each of the m sites located on them will be

$$F = \frac{1}{ma}\frac{\partial \psi}{\partial r}, \tag{22}$$

where a is the distance between two successive radii. Again we use a discrete approximation for the derivative and evaluate the adimensional force per monomer $\frac{a\beta F}{\langle N \rangle}$, at the critical condition, which is given by

$$f(r+1/2, \omega) = \frac{2[x_c(r+1,\omega) - x_c(r,\omega)]}{m[x_c(r+1,\omega) + x_c(r,\omega)]}. \tag{23}$$

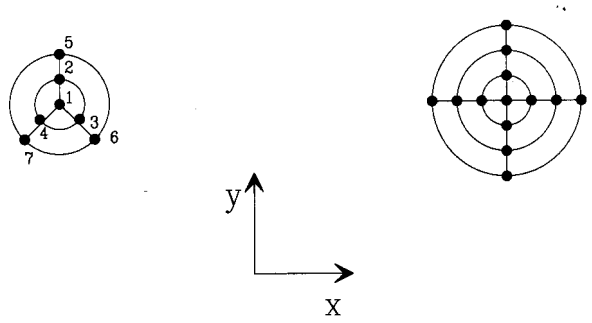

Figure 7. Two examples of crossections for cylindrical pores: (a) $r = 2$, $m = 3$, with the sequential numbering of sites shown; (b) $r = 3$, $m = 4$.

We will briefly show how the properties of *ideal* chains confined in the pores defined above may be studied. For this we define a set of $r+1$ partial partition functions $g_l(i), i = 0, 1, \ldots, r$. In $g_l(i)$ the contributions of all chains with l steps ($l-1$ monomers) whose final monomer is located at a distance i of the center of the pore are included. It is then easy to write done the recursion relations for the $g_l(i)$, which are

$$\begin{aligned} g_{l+1}(0) &= x_0[2g_l(0) + mg_l(1)]; \\ g_{l+1}(i) &= x_i[4g_l(i) + g_l(i+1) + g_l(i-1)], i = 1, 2, \ldots, r-1; \\ g_{l+1}(r) &= x_r[4g_l(r) + g_l(r-1)]. \end{aligned} \tag{24}$$

If the initial monomer is placed at the center of the pore, we have

$$g_0 i = x_0 \delta_{i,0}. \tag{25}$$

As usual, we may define the partition functions

$$G(i) = \sum_{l=0}^{\infty} g_l(i), \tag{26}$$

which are the solution of a set of $r+1$ linear equations

$$\sum_{j=1}^{r+1} [A(i,j) - \delta_{i,j}] G(j) = -g_0(i). \tag{27}$$

The matrix A in this case has a very simple structure, which is

$$A = \begin{pmatrix} 2x_0 - 1 & mx_0 & 0 & 0 & \dots & 0 & 0 & 0 \\ x_1 & 4x_1 & x_1 & 0 & \dots & 0 & 0 & 0 \\ 0 & x_2 & 4x_2 & x_2 & \dots & 0 & 0 & 0 \\ \vdots & \vdots & \vdots & \vdots & \vdots & \vdots & \vdots & \vdots \\ 0 & 0 & 0 & 0 & \dots & x_{r-1} & 4x_{r-1} & x_{r-1} \\ 0 & 0 & 0 & 0 & \dots & 0 & x_r & 4x_r \end{pmatrix} . \quad (28)$$

Due to the band structure of the matrix some properties of the model may be calculated analytically [30].

To study the properties of self-avoiding chains in the pores, we generated the crossection configurations and the polynomials which are the elements of the transfer matrix. As an example, we show some results for $m = 3$. Since at each additional value of the radius r the number of sites in the crossection is increased by m, the number of crossection configurations grows very fast with r, limiting the cases we could consider. For $r = 1, 2, 3$ we found $N_c = 16, 532, 26200$ and $N_s = 5, 108, 4530$, respectively. So, we limited ourselves to a maximum value $r = 2$. As in the cases of chains in strips, some possible configurations are not connected to any other in the transfer matrix and therefore may be eliminated. But, unlike to what happens for chains in strips, these configurations are not obvious *a priori*, so we detected them after the transfer matrix was obtained. Such configurations do not occur for $r = 1$ and for $r = 2$ their elimination reduced N_c to 531 and N_s to 105.

In Fig. 8 the densities for ideal and self-avoiding chains in the pore are shown for $r = 2$ and $m = 3$ as functions of ω. Although differences are apparent between both cases, they are relatively smaller than the ones observed in the case of chains in strips. This is expected since the coordination numbers of the sites in the pores are larger than the ones of the corresponding sites in the strips, and thus the self avoidance constraint is expected to have a smaller influence on the results for chains in pores. Finally, Fig. 9 displays the results obtained for the force on the walls for $r = 2, m = 3$. Again we notice that, similar to what was found for the strips, the force vanishes at a lower value of ω for ideal chains than it does for self-avoiding chains.

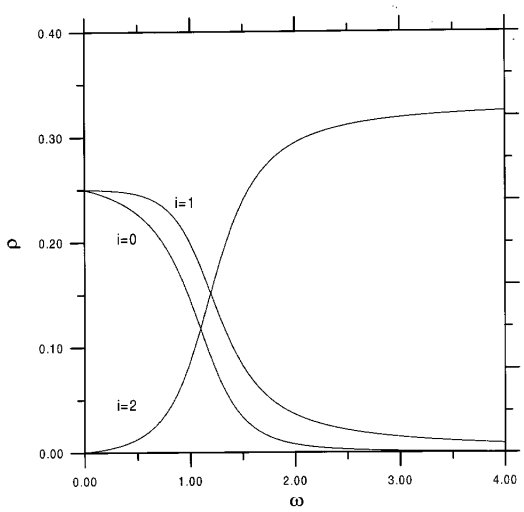

(a)

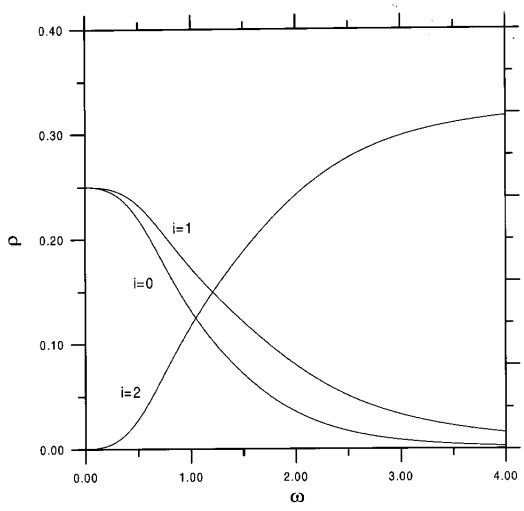

(b)

Figure 8. Fractions of monomers $\rho(i)$ for chains placed in cilindrical pores with $r = 2$ and $m = 3$. For $i > 0$ the fractions indicated correspond to monomers located at one of the m sets of sites situated at a distance i from the center. Results for (a) ideal and (b) self avoiding chains are shown.

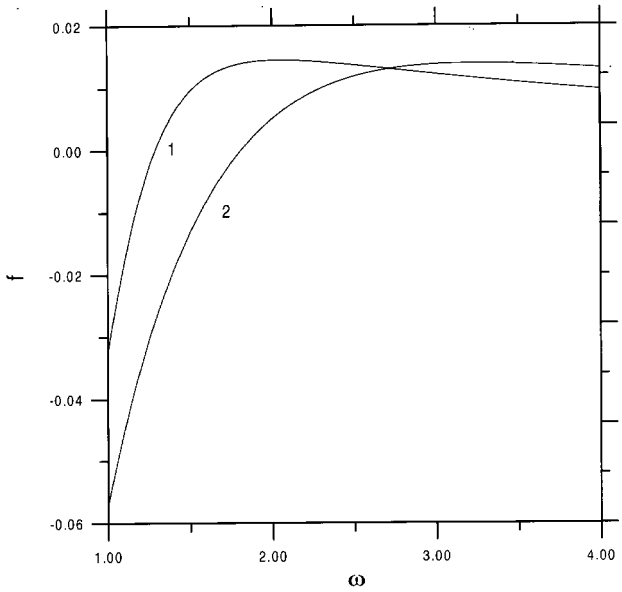

Figure 9. Force on the wall for cylindrical pores with $r = 2$ and $m = 3$. Curve 1 corresponds to ideal and curve 2 to self avoiding chains.

V Discussion and final comments

We studied the properties of ideal and self-avoiding chains in strips and pores, concentrating on the spatial distribution of monomers and on the tension on the walls. It should be stressed that the solution of statistical mechanical models in confined geometries, particularly on strips or on the surface of cylinders, is not new. The main interest in such studies is to use finite size scaling in order to provide information on the behavior of the two-dimensional models from the solution of a sequence of one-dimensional models [31]. Also, scaling arguments have been applied very successfully to confined polymers [32], but it should be noticed that these arguments usually lead to monotonical behavior of the thermodynamic properties with the size of the system. Our results show their most interesting features at sizes below the ones where finite size scaling is valid. This is clear if we consider the tension on the walls of the strips, which display equilibrium points at low values of N_p.

To our knowledge, there are no experimental results regarding the distribution of monomers for chains confined in pores or strips. The tension on plates with polymers in solution has been measured [33], being repulsive at low plate separation with a weak attractive tail as the separation increases, in qualitative agreement with the results for ideal chains. So, at least within the precision of the measurements, no unstable equilibrium point was found. Oscillating forces have also been reported [34], but only for monodisperse melts with rather low numbers of monomers (N equal to 20 and 65), and thus no comparison can be made with the present calculations. In principle, it would be possible to study the behavior of monodisperse melts with techniques similar to the ones used above, but with a transfer matrix which will grow very fast with the number of monomers.

Acknowledgments

We acknowledge partial financial support by the Brazilian agencies FINEP and CNPq, as well as a critical reading of the manuscript by Kleber D. Machado.

References

[1] P. J. Flory, *Principles of Polymer Chemistry*, Cornell University Press (1953).

[2] B. Duplantier, J. Stat. Phys. **54**, 581 (1989)

[3] P.-G. de Gennes, Phys. Lett. A **38**, 339 (1972)

[4] P.-G. de Gennes, *Scaling Concepts in Polymer Physics*, third printing, Cornell University Press (1988).

[5] P. Gujrati, Phys. Rev. B **31**, 4375 (1985); Phys. Rev. Lett. **55**, 1161 (1985).

[6] J. C. Wheeler, J. F. Stilck, R. G. Petschek and P. Pfeuty, Phys. Rev. B **35**, 284 (1987).

[7] J. F. Nagle, C. S. O. Yokoi, and S. M. Bhattacharjee in *Phase Transitions and Critical Phenomena*, vol. 13, ed. by C. Domb and J. L. Lebowitz, Academic Press (1989).

[8] D. Stauffer, Phys. Repts. **54**, 1 (1979).

[9] P. W. Kasteleyn and C. M. Fortuin, J. Phys. Soc. Japan Suppl. **26**,11 (1969), and Physica **57**, 536 (1974). See also J. W. Essam in *Phase Transitions and Critical Phenomena*, vol 2, ed. by C. Domb and M. S. Green, Academic Press (1972).

[10] H. N. V. Temperley and M. E. Fisher, Phil. Mag. **6**, 1061 (1961); P. W. Kasteleyn, Physica **27**, 1209 (1961) and J. Math. Phys. **4**, 287 (1963).

[11] J. C. Wheeler, S. Kennedy and P. Pfeuty, Phys. Rev. Lett. **45**, 1748 (1980); J. C. Wheeler and P. Pfeuty, Phys. Rev A **24**, 1050 (1981).

[12] P. M. Pfeuty and J. C. Wheeler, Phys. Rev. A **27**, 2178 (1983).

[13] B. Derrida, J. Phys. A **14**, L5 (1981).

[14] A. R. Conway and A. J. Guttmann, Phys. Rev. Lett. **77**, 5284 (1996).

[15] B. Nienhuis, Phys. Rev. Lett. **49**, 1062 (1982); see also B. Nienhuis in *Phase Transitions and Critical Phenomena*, vol 11, ed. by C. Domb and J. L. Lebowitz, Academic Press (1987).

[16] A. J. Guttmann and I. G. Enting, Phys. Rev. Lett. **76**, 344 (1996).

[17] J. F. Stilck and J. C. Wheeler, J. Stat. Phys. **46**, 1 (1987); J. Stilck and M. J. de Oliveira, Phys. Rev. A **42**, 5955 (1990); E. Botelho and J. F. Stilck, Phys. Rev. E **48**, 723 (1993).

[18] V. Privman and N. M. Švarkić, *Direct Models for Polymers, Interfaces and Clusters: Scaling and Finite Size Properties*, Lecture Notes in Physics, Springer, Berlin (1989).

[19] K. De'Bell and T. Lookman, Rev. Mod. Phys. **65**, 87 (1993).

[20] K. Binder in *Phase Transitions and Critical Phenomena*, vol. 8, ed. by C. Domb and J. L. Lebowitz, Academic Press (1983).

[21] R. J. Rubin, J. Chem. Phys. **43**, 2392 (1965).

[22] P. Serra and J. F. Stilck, Europhys. Lett. **17**, 423 (1992); Phys. Rev. E **49**, 1336 (1994).

[23] E. Eisenriegler, K. Kremer and K. Binder, J. Chem. Phys. **77**, 6286 (1982); E. Eiseriegler, J. Chem. Phys. **79**, 1052 (1983).

[24] I. Guim and T. Burkhardt, J. Phys. Am**22**, 1131 (1989).

[25] D. Zhao, T. Lookman and K. De'Bell, Phys. Rev. A **42**, 4591 (1990).

[26] J. M. Hammersley and S. G. Whittington, J. Phys. A **18**, 101 (1985); S. G. Whittington and C. E. Soteros, Israel J. of Chem. **31**, 127 (1991).

[27] J. F. Stilck, Europhys. Lett. **40**, 19 (1997); Physica A **257**, 233 (1998).

[28] J. F. Stilck and K. D. Machado, Eur. Phys. J., accepted (1998).

[29] P. Serra, doctoral thesis (USP - Brazil) (1991).

[30] E. A. DiMarzio and R. J. Rubin, J. Chem. Phys. **55**, 4318 (1971).

[31] M. N. Barber in *Phase Transitions and Critical Phenomena*, vol. 8, ed. by C. Domb and J. L. Lebowitz, Academic Press (1983).

[32] V. Privman, Phys. Rev. B **32**, 520 (1985).

[33] K. Ingersent, J. Klein, and P. Pinkus, Macromolecules **19**, 1374 (1986).

[34] J. N. Israelachvili and S. J. Kott, J. Chem. Phys. **88**, 7162 (1988).